



HAL
open science

Spectroscopic evidence and mechanistic insights on dehydrofluorination of PVDF in alkaline medium

Jeet Sharma, Cedric Totee, Vaibhav Kulshrestha, Bruno Ameduri

► To cite this version:

Jeet Sharma, Cedric Totee, Vaibhav Kulshrestha, Bruno Ameduri. Spectroscopic evidence and mechanistic insights on dehydrofluorination of PVDF in alkaline medium. *European Polymer Journal*, 2023, 201, pp.112580. 10.1016/j.eurpolymj.2023.112580 . hal-04281670

HAL Id: hal-04281670




<https://hal.science/hal-04281670v1>

Submitted on 13 Nov 2023

HAL is a multi-disciplinary open access archive for the deposit and dissemination of scientific research documents, whether they are published or not. The documents may come from teaching and research institutions in France or abroad, or from public or private research centers.

L'archive ouverte pluridisciplinaire **HAL**, est destinée au dépôt et à la diffusion de documents scientifiques de niveau recherche, publiés ou non, émanant des établissements d'enseignement et de recherche français ou étrangers, des laboratoires publics ou privés.

Spectroscopic evidence and mechanistic insights on dehydrofluorination of PVDF in alkaline medium

Jeet Sharma ^{1,2,3} , Cedric Totee ¹, Vaibhav Kulshrestha ^{2,3} , Bruno Ameduri ^{1*} 

¹ Institute Charles Gerhardt, University of Montpellier, CNRS, ENSCM, 34293, Montpellier, France

² Council of Scientific and Industrial Research - Central Salt and Marine Chemicals Research Institute (CSIR-CSMCRI), Membrane Science and Separation Technology Division, Bhavnagar, India-364002.

³ Academy of Scientific and Innovative Research (AcSIR), Ghaziabad, Uttar Pradesh, India-201002.

Corresponding author: bruno.ameduri@enscm.fr

Abstract

This study presents newer insights on the dehydrofluorination of poly(vinylidene fluoride), PVDF, in alcoholic sodium hydroxide using infrared (IR), Raman and nuclear magnetic resonance (¹H and ¹H {¹⁹F}) spectroscopies. Details on the reactivity of phases and site selectivity of different orientations viz head-to-tail and tail-to-tail is comprehensively examined using IR/Raman and NMR (1D and 2D), respectively. The α -phase is prominently involved in dehydrofluorination and transforms into the more electroactive β -phase. ¹H-NMR spectra highlight that the tail-to-tail addition of PVDF is not disturbed and remains unaffected during dehydrofluorination reaction. Furthermore, ¹H-¹⁹F heteronuclear correlation spectroscopy (Hetero COSY) clearly evidences the formation of the -(CH=CF)- double bond in dehydrofluorinated PVDF. Moreover, detailed mechanistic insights of dehydrofluorination reaction and possible internal crosslinking during the chemical transformation is presented.

Keywords: Alkaline dehydrofluorination; fluorinated polymer; mechanism; PVDF conformation; IR, Raman and NMR spectroscopy.

1. Introduction

With global market of approx. \$ 8.0 billion and still intent to grow, the fluoropolymers are important class of macromolecules [1-5]. Attributed to outstanding bond dissociation stability of C-F linkage and fine malleable properties, poly(vinylidene fluoride) (PVDF) is the most important fluorinated homopolymer and produced as the second highest utility material for advanced scientific research after poly(tetrafluoroethylene) (PTFE) [6]. In recent years, PVDF have been gaining sustained surveillance due to its ease in functional modifications as high-performance engineered materials for various crystalline piezoelectric components (attributed to the special dipole orientations), ion-exchange membranes for water-energy nexus viz water desalination, polyelectrolyte fabrication for fuel cell/batteries and in anti-aging/flame retardant coating-based applications [1-4, 7, 8]. Like PTFE [6], PVDF can sustain and endure aggressive conditions viz high temperature, ageing, chemical and oxidative degradation and exhibit relevant physical properties like electroactive properties, gas barrier attributes and friction resistance, which are of significant applicability [1-5, 7, 9, 10].

However, a major drawback of these niche polymers (i.e., PVDF and VDF copolymers) is their sensitivity and reactivity to alkaline conditions ($\text{pH} > 11.0$), especially the caustic and hydroxides [9-15]. Since, no explanations on the driving force for dehydrofluorination of PVDF is present in literature, the plausible explanation to the feasibility is more onto the thermodynamic considerations related to overall entropy increase during dehydrofluorination reaction. Moreover, once the unsaturation is obtained, the reaction is autocatalyzed due to improved reactivity of adjacent H-atoms in dehydrofluorinated PVDF [15]. Interestingly, this chemical reactivity at high pH offers two-fold merits: on the one hand, various scientific groups have been involved in taking advantage of unsaturated site induction for its structural and chemical property modifications [16-20]. On the other hand, it offers avenues to satisfy and explore versatile applicability for energy and environment applications [21, 22]. Various reports have explored the chemical transformation of PVDF by reacting with amines [17, 23, 24], thiol [18], alkali metal carbonates [25], alkali metal hydroxides [11], in presence of phase transfer catalyst [15, 26], and under thermal degradation [27]. In addition, studies concerning the crosslinking of PVDF is also reported in presence of basic nucleophiles, as telechelic bisphenol, peroxide, etc [28, 29]. For instance, Kise and Ogata [11] investigated the dehydrofluorination of PVDF in the presence of quaternary ammonium and

phosphonium halides as phase transfer catalysts (PTC). The functionality and chemical transformation of obtained product was evidenced using infrared spectroscopy (IR) and corresponding air stable conjugated polyene type chemical structures were observed. Ahmed et al. [15, 26] characterized the dehydrofluorination of PVDF by IR and Raman spectroscopy techniques and the study confirms that the sodium hydroxide in propan-2-ol PTC alters the reaction pathway. The source of proton in the dehydrofluorination of PVDF is propan-2-ol. In addition, the principle of group theory was applied and different modes of vibration were probed in alkali modified PVDF. Girish et al. [30] studied the density functional theory on PVDF and dehydrofluorinated PVDF. The structural studied on dehydrofluorinated material states that the stability of material is improved and the polymer chains acquire more planar conformation. Wang et al. [17] carried out the dehydrofluorination of PVDF using ethylene diamine as a dehydrofluorination reagent. The nature of the double bond was evidenced using x-ray photoelectron spectroscopy (in 285 eV region of XPS C (1s) deconvoluted spectrum) and fraction of C=C was explained with dehydrofluorination time showing improved piezoelectric properties in portable electronic devices. Cozzarini and Schmid [31] described the mechanical instability of the PVDF pipes in alkaline conditions. These observations were corroborated based on the optical imaging and microscopy followed by IR spectroscopy analysis. Moreover, studies are claimed for dehydrohalogenation of copolymers and *ter*-polymers. For instance, Tan et al. [32] explored the dehydrofluorination reaction (E_2 elimination reaction) in poly(VDF-*co*-CTFE) copolymer using different tertiary amines such as trimethyl amine, tri (n-butyl) amine, hexamethylene tetramine and N,N-dimethyl aniline. The 1H - and ^{19}F -NMR spectroscopy suggests the formation of double bond by signals in the 6.0 to 6.5 ppm range in the 1H -NMR spectrum. Li and Liao [33, 34] conducted the evaluation of various VDF based copolymer and terpolymer viz poly(VDF-*co*-HFP) and poly(VDF-*ter*-HFP-*ter*-TFE), respectively and proposed mechanisms from the comprehensive assessment on dehydrofluorination. Ross et al. [12] evidenced the surface modification of PVDF in 12 M NaOH electrolyte using XPS, secondary ion mass spectrometry (SIMS) and Raman spectroscopy, and they proposed a corresponding oxidation and dehydrofluorination mechanism.

Evidently, several studies on the potential utilization of unsaturation in PVDF have been reported in the recent years [16-20]. However, the studies remained limited to the achievements of functional interconversion for various applications only and the spectroscopic characterizations have not been deeply

investigated except for the X-ray photoelectron, infrared, Raman spectroscopies and mass spectrometry. Since the literature is rich in what transformation happens with various reagents, it is rather more important to focus on how it happens and find evidences on time dependent modifications and reactivity of PVDF in efficient alcoholic alkaline media. Thus, it is worth performing an in-depth investigation on the site selectivity during dehydrofluorination of PVDF and to present extended insights on phase transformations using IR and Raman analyses. Moreover, to the best of our knowledge, this manuscript is first ever report on finding the actively

Experiment	Experiment time (h)	NaOH conc. (Vol. added in mL) [in Molar, (mL)]	Experimental NaOH concentration in reaction flask [in Molar]	Sample code
-------------------	----------------------------	-------------------------------------------------------	---------------------------------------------------------------------	--------------------

involved orientation in PVDF during dehydrofluorination by complimentary 1D and 2D NMR spectroscopy.

Table 1. Dehydrofluorination experiments of PVDF performed with different concentrations of NaOH/propan-2-ol alkaline reagent.

1	2	0.25 (5.0)	0.0225	DHF-PVDF 2h (0.25 M)
2	4	0.25 (5.0)	0.0225	DHF-PVDF 4h (0.25 M)
3	8	0.25 (5.0)	0.0225	DHF-PVDF 8h (0.25 M)
4	12	0.25 (5.0)	0.0225	DHF-PVDF 12h (0.25 M)
5	24	0.25 (5.0)	0.0225	DHF-PVDF 24h (0.25 M)
6	2	0.5 (5.0)	0.0450	DHF-PVDF 2h (0.5 M)
7	4	0.5 (5.0)	0.0450	DHF-PVDF 4h (0.5 M)
8	8	0.5 (5.0)	0.0450	DHF-PVDF 8h (0.5 M)
9	12	0.5 (5.0)	0.0450	DHF-PVDF 12h (0.5 M)
10	24	0.5 (5.0)	0.0450	DHF-PVDF 24h (0.5 M)
11	2	1.0 (5.0)	0.0900	DHF-PVDF 2h (1 M)
12	4	1.0 (5.0)	0.0900	DHF-PVDF 4h (1 M)
13	8	1.0 (5.0)	0.0900	DHF-PVDF 8h (1 M)
14	12	1.0 (5.0)	0.0900	DHF-PVDF 12h (1 M)
15	24	1.0 (5.0)	0.0900	DHF-PVDF 24h (1 M)

Note: All the reactions are carried out in open air environment with 10 w/v% of PVDF/DMAc polymer solution (50 mL) at 25°C. The experimental molar concentration was calculated using the final volume of functionally modified polymer solution.

2. Materials and Methods

2.1. Materials

Polyvinylidene fluoride (Kynar 301-F, PVDF, $M_n = \square 350 \text{ kg mol}^{-1}$) was supplied by Arkema, France (approx. MFI range of 2.0-6.0 g per 10 min at $\square 230 \text{ }^\circ\text{C}$). *Solvent:* Dimethyl acetamide (DMAc) and propan-2-ol was purchased from Honeywell Riedel-de-Haën™. *Base:* Sodium hydroxide was procured from Fluka analysis and used as dehydrofluorination reagent for unsaturation site induction.

2.2. Dehydrofluorination of PVDF

Dehydrofluorination was carried out in solution phase using sodium hydroxide /propan-2-ol solution prepared at $30 \pm 2 \text{ }^\circ\text{C}$. In brief, the PVDF powder was dissolved in DMAc to make 10.0 w/v % clear homogenous solution. To such an obtained PVDF/DMAc polymer solution, the desired quantity of sodium hydroxide (i.e., 0.25 M, 0.5 M and 1.0 M) solution was added maintaining the polymer to alkali ratio of 1.0:0.1 v/v. The dehydrofluorination was visualised initially with chromic transition from transparent to light green to dark brown within initial 60 s. All the dehydrofluorination reactions were carried out at $25 \pm 1 \text{ }^\circ\text{C}$ over the variable

times viz 2 h, 4 h, 8 h, 12 h and 24 h, respectively. The reaction at each interval was quenched by precipitation of the product in cold deionized water repeatedly to remove excess DMAc and purify the polymer. Finally, the obtained dehydrofluorinated PVDF (DHF-PVDF) fibers were allowed to dry in vacuum oven at 60 °C to discard any residual solvent. **Table 1** illustrates experimental details adopted under study for dehydrofluorination of PVDF. This reaction was performed in different conditions by varying the NaOH concentration and reaction time. For example, the NaOH concentration of 0.25 M was observed to be low and 1.0 M NaOH was high enough to acquire dehydrofluorination. Concerns regarding the experimental NaOH is also highlighted which is important to understand experimental conditions in one-pot. Moreover, the reaction using 0.5 M NaOH for 12 h was considered the most appropriate one due to the retention in mechanical stability and satisfactory solubility in acetone.

PVDF ¹H-NMR (400MHz): 1.04 ppm ($\text{CH}_3\text{CH}_2\text{CF}_2^-$, triplet, $^3J_{\text{HH}} = 7.5$ Hz), 1.81 ppm ($-\text{CH}_2\text{CF}_2\text{CH}_3$, triplet, $^3J_{\text{HF}} = 10$ Hz), 2.37 ppm ($-\text{CF}_2\text{CH}_2\text{CH}_2\text{CF}_2^-$, broad triplet, $^3J_{\text{HH}} = 15.5$ Hz), 2.95 ppm to 2.97 ppm ($-\text{CH}_2\text{CF}_2\text{CH}_2\text{CF}_2^-$, quintet, $^3J_{\text{HF}} = 10$ Hz) and 6.32 ppm ($-\text{CH}_2\text{CF}_2\text{H}$, triplet ($^2J_{\text{HF}} = 45$ Hz) of triplets ($^3J_{\text{HH}} = 7$ Hz)). [35, 36]

DHF-PVDF ¹H-NMR (400MHz): 1.04 ppm ($\text{CH}_3\text{CH}_2\text{CF}_2^-$, triplet, $^3J_{\text{HH}} = 7.5$ Hz), 1.81 ppm ($-\text{CH}_2\text{CF}_2\text{CH}_3$, triplet, $^3J_{\text{HF}} = 10$ Hz), 2.37 ppm ($-\text{CF}_2\text{CH}_2\text{CH}_2\text{CF}_2^-$, broad triplet, $^3J_{\text{HH}} = 7$ Hz), □ 2.82 ppm ($-\text{CF}_2\text{CH}_2\text{COCH}_2\text{CF}_2$, singlet), 2.95 ppm (solvent water), 2.97 ppm ($-\text{CH}_2\text{CF}_2\text{CH}_2\text{CF}_2^-$, quintet, $^3J_{\text{HF}} = 10$ Hz), 5.38 ppm ($-(\text{CH}_2-\text{CH}=\text{CF}-\text{CH}_2)_3-$, broad), □ 6.0 ppm ($-\text{CF}_2-\text{CH}=\text{CFCH}_2^-$, complex multiplet, $^3J_{\text{HF}} (\text{-CF}_2\text{-CH-}) = 10$ Hz and $^3J_{\text{HF}} (\text{-CF=CH-}) = 12$ Hz) and 6.32 ppm ($-\text{CH}_2\text{CF}_2\text{H}$, triplet ($^2J_{\text{HF}} = 45$ Hz) of triplets ($^3J_{\text{HH}} = 7$ Hz)).

2.3. Spectroscopic characterization

The dehydrofluorination was probed with the ¹H-NMR and ¹H {¹⁹F(Spectrometer: Bruker Avance III HD, 400 MHz) spectrum of pristine PVDF and alkali modified PVDF in Acetone-d₆ as the solvent. All 1D NMR measurements were carried out at a scan rate of 256 with line broadening normalized to 2.0 Hz using Bruker TopSpin 4.1.4 version of software. Experimental conditions for probing the proton nuclei is as follows; tilt angle at 30°, acquisition time = 4 s, relaxation time = 1 s and a pulse width of 11.7 μs. Concerning ¹⁹F decoupling, globally optimized alternating phase rectangular pulse (GARP) sequence was applied during acquisition with a pulse

width of 90 μ s. Two-dimensional Heterocosity $^1\text{H}/^{19}\text{F}$ spectra were acquired providing correlations between protons and fluorine without νJ limits. 2D $^1\text{H}/^{19}\text{F}$ Heterocosity single quantum coherence (SQC) experiments were carried out with a spectral width of 4kHz for ^1H with a center at 1200 Hz and 22.5 kHz for ^{19}F with a center at -37.5 kHz. Acquisition time was set to 0.05 s in the first dimension and 0.5 s in the second. Relaxation delay was 1 s, and number of scans was set to 64 according to signal/noise and phase correction. A double Fourier transform (FT) was provide (8K \times 4K) without linear prediction in both dimensions.

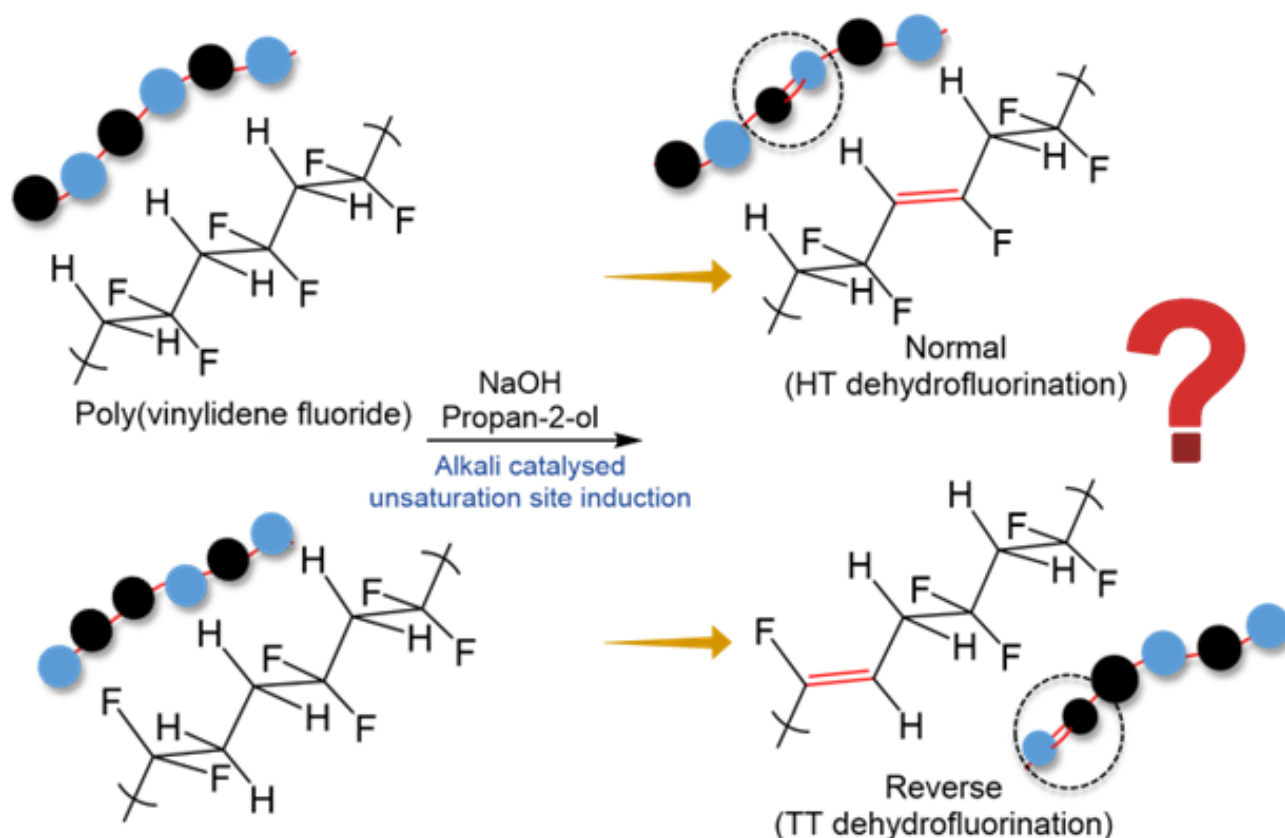
The prominent stretching and bending modes of vibration in PVDF and DHF-PVDF was further confirmed by attenuated total reflectance infrared spectroscopy (ATR-IR) in the finger print region using Thermo Scientific NICOLET iS50 ATR-IR spectrometer performing background calibrations at each record of 32 scans per sample.

The Raman spectra were obtained using Horiba Jobin Yvon-LabRAM ARAMIS spectrophotometer with charged coupled device (CCD) cooled detector employing the 633 nm incident laser (Number of scans = 100 and acquisition parameter = 2) in full 4000-400 cm^{-1} range.

3. Result and Discussion

In the past years, the change in electrochemical and dielectric properties of PVDF after dehydrofluorination has been reported [9, 10, 37]. The different phases in PVDF are responsible for the fine-tuning of properties in this niche fluoropolymer [37, 38]. For instance, from the α -, β -, γ -, δ - and ϵ -phases of PVDF, the pure β -phase is responsible for improvements in electroactive feature and overall softness of the PVDF for functional processing making these materials important (e.g., piezoelectric device, actuators, etc.) [38-40]. Moreover, the formation of internal double bonds due to dehydrofluorination in PVDF gains considerable interest for various applications through strategic functional modifications [22, 41]. Studies by Ross et al. [12] suggest different steps viz dehydrofluorination and oxygenation during a chemical degradation of PVDF in alkaline media [12]. In stark contrast, Wang et al. [17] reported that C-F bonds are difficult to activate but with methylene units in the main chain, the system attains a feasible reactive state to form double bonds (or conjugate double bonds). The reaction is so sensitive that even 0.1% of

unsaturation causes significant change in polymer colour. Prima facie, there is no report discussing on the prominent region of the ^1H -NMR spectra (i.e., tail-to-tail and head-to-tail region) that can provide useful insights on the chemical changes (**Scheme 1**). Thus, it is important to validate the detailed spectroscopic studies on the selective dehydrofluorination site of PVDF and elaborate the mechanistic insight in present literature.



Scheme 1. Schematic illustration with scope to decipher the potential orientation for the dehydrofluorination reaction of PVDF. What is the missing link to determine principal reaction site (Head-to-Tail [HT] (up) or Tail-to-Tail [TT] (bottom)?

The resulting dehydrofluorinated PVDFs are characterized by IR, Raman, ^1H and ^{19}F spectroscopy.

3.1. Infrared spectroscopy results and influence on PVDF phase

Figure 1a represents the ATR-IR spectra of PVDF and dehydrofluorinated PVDF in fingerprint region and the results were studied based on the change in chemical functionalities and phase, respectively. In PVDF, mostly the spectrum between 400 cm^{-1} to 1500 cm^{-1} corresponds to the stretching/bending frequencies of single

bonds [42]. Cai et al. [43] reported that different treatments methods viz electrospinning and solvent casting influence phases of PVDF differently. In addition, three prominent variables of the bands are observed in the ATR-IR spectra viz, the common peaks (describing all phases), exclusive peaks (specific to only one phase) and mutually co-existing peaks (showing the co-existence of two phases) related to α -, β -, γ -phases or combination of these phases. Lanceros-Mendez et al. [38] reviewed on the phase change behaviour in PVDF under the influence of applied mechanical stress. The results were explained based on the change in the phase peaks and enthalpy of material using FT-IR spectrum and differential scanning calorimetry, respectively. However, the correlation of modes of vibration and phase detected for each vibration is assigned with respect to the proposed mechanism of dehydrofluorination explained in section 3.3.

Fingerprint region of ATR-IR spectra: In the ATR-IR spectrum of PVDF (**Figure 1a**), the vibrational frequencies at 763 cm^{-1} and 794 cm^{-1} corresponds to the C-F in-plane bending or rocking mode of bending exclusively for the α -phase [42]. Evidently, over dehydrofluorination of PVDF, the signal attributed to this α -phase (between 750 cm^{-1} - 800 cm^{-1}) disappears while a new broad absorption band near 840 cm^{-1} corresponding to the $-\text{CH}_2-$ rocking mode and difluoromethylene ($-\text{CF}_2-$) asymmetric stretching mode for the out of phase (i.e., β -phase) was observed [44]. In addition, an overlapping of signal in the proximity of 840 cm^{-1} is assigned for the tri-substitutions in dehydrofluorinated PVDF motifs for the $-(\text{CF}_2\text{-CH}=\text{CF-CH}_2)-$ region. The signal at 872 cm^{-1} corresponds to the mutually co-existing β - and γ -phase in PVDF and illustrates absolute retention in its band behaviour after dehydrofluorination. This suggests that the α -phase is the participating phase. Moreover, the new subtle band at 1624 cm^{-1} , which was not obtained in the pristine PVDF material, evidences the formation of double bond in the alkali treated PVDF material [45] (**Figure 1b**).

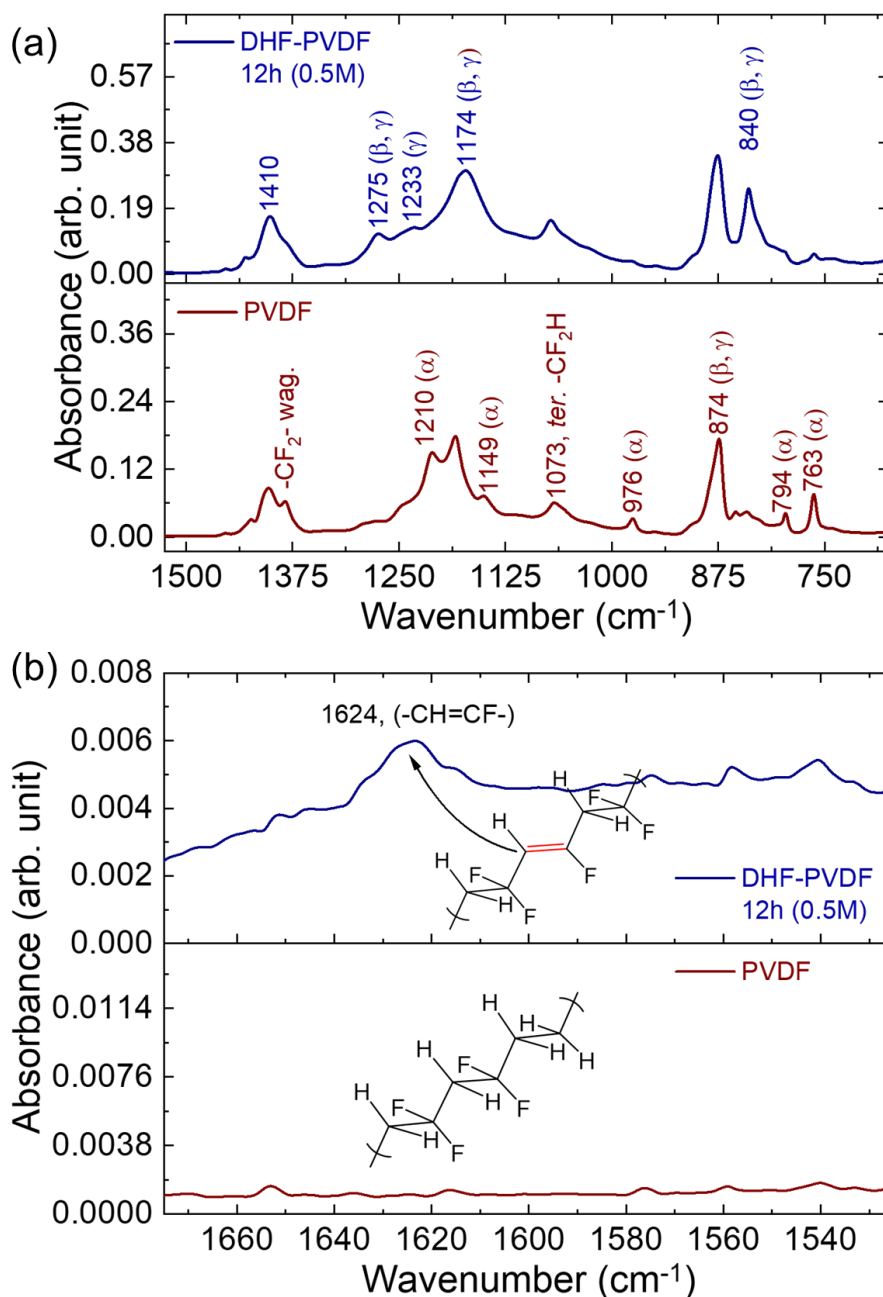


Figure 1. (a) Expansion of $1525\text{ cm}^{-1} - 620\text{ cm}^{-1}$ zone from the ATR-IR spectra of PVDF (bottom) and dehydrofluorinated PVDF (up) after treating with 0.5 M NaOH for 12 h at $25\text{ }^{\circ}\text{C} \pm 1\text{ }^{\circ}\text{C}$ (Experiment 9, Table 1) and b) ATR-IR spectra of PVDF (bottom) and dehydrofluorinated PVDF (up) in the olefin ($-\text{CH}=\text{CF}-$) region (here, the peak intensity is of order $\times 10^{-3}$ arb. unit).

In comparison to other peaks, the weak intensity of olefin stretching modes at 1624 cm^{-1} might be attributed due to the applicability of “*mutual co-exclusion principal*” [15]. The absorption signal at 1210 cm^{-1} for the difluoromethylene stretching mode in α -phase of PVDF confers that the PVDF strongly exists in α -phase with the traces of β -phase [43].

Table 2. Correlation of the principal modes of vibration and change in corresponding phases from ATR-IR result of PVDF and dehydrofluorinated PVDF [39-42, 44].

Absorption peak in ATR-IR spectrum (cm ⁻¹)	Poly(vinylidene fluoride), (PVDF) [vibration mode, phase]	Dehydrofluorinated PVDF, (DHF-PVDF) [vibration mode, phase]
763.0	[-C-F (in-plane bending or rocking), α -phase] <i>excl.</i>	-* ₋
794.0	[-C-F (in-plane bending or rocking), α -phase] <i>excl.</i>	-* ₋
840.0	-* ₋	[-CH ₂ - rocking vibration and -CF ₂ - <i>v_{asym.}</i> mode, β - and γ -phase)] <i>mutually co-existing peaks</i>
872.0	[C-F band vibration, β - and γ -phase)] <i>mutually co-existing peaks</i>	[C-F band vibration, β - and γ -phase)] <i>mutually co-existing peaks (ret)</i>
976.0	[C-C stretching vibration, α -phase] <i>excl.</i>	[traces of C-C stretching vibration, α -phase] <i>disappeared, excl.</i>
1073.0	[terminal -CF ₂ H group vibration, <u>UD</u>]	[terminal -CF ₂ H group vibration, <u>UD</u>] <i>(ret)</i>
1150.0	[C-F stretching vibration, α -phase]	-* ₋
1174.0	[-CF ₂ - stretching vibration mode, β - and γ -phase)] <i>mutually co-existing peaks</i>	[-CF ₂ - stretching vibration mode, β - and γ -phase)] <i>mutually co-existing peaks (ret)</i>
1210.0	[-CF ₂ - stretching vibration mode, α -phase]	-* ₋
1234.0	[-CF ₂ - stretching vibration mode, γ -phase]	[-CF ₂ - stretching vibration mode, γ -phase] <i>(ret)</i>
1275.0	No traces of any peak.	[C-F stretching, β -phase] <i>excl.</i>
1380.0	[-CF ₂ - wagging out-of-plane, <u>UD</u>]	-* ₋
1401.0 and 1403.0	[-CH ₂ - wagging out-of-plane, β - and γ -phase)] <i>mutually co-existing peaks</i>	[-CH ₂ - wagging out-of-plane, β - and γ -phase)] <i>mutually co-existing peaks (ret)</i>
1624.0	No traces of any peak.	[C=C bond vibration, β -phase] <i>excl.</i>

Abbrv. = peak disappears in PVDF after dehydrofluorination (-*₋), exclusive peak (*excl.*), asymmetric stretching vibration (*v_{asym.}*), mutually co-existing peaks (*mutually co-existing peaks*), retention of peak (*(ret)*), undetermined (UD).

In stark contrast, after dehydrofluorination, the vibration band at 1275 cm^{-1} corresponding exclusively to the β -phase for C-F out-of-plane deformation [46] and the vanishing of absorption band near 976 cm^{-1} (attributed to the C-C stretching mode of vibration in α -phase) strongly corroborates that the β -phase becomes dominant which is crucial for electroactive applications.

Another interesting feature is that the peak at 1073 cm^{-1} corresponding to the terminal $-\text{CF}_2\text{H}$ group remains unaffected showing that the dehydrofluorination occurs in between the chains [47, 48]. This observation is also confirmed by the presence of triplet ($^2J_{\text{HF}}=45$ Hz) of triplets ($^3J_{\text{HH}}=7$ Hz) centered at \square 6.3 ppm region in $^1\text{H-NMR}$ spectrum of dehydrofluorinated PVDF. This suggests that the dehydrofluorination of PVDF is accompanied by phase changes from its original state and most preferably attains the β -phase which possesses high dipole moment in comparison to the other phases. **Table 2** illustrates the relation between phases and corresponding modes of vibration for $-\text{CH}_2-$, $-\text{CF}_2-$, C-H and C-F bonds.

The results confirm a strong correlation between the vanishing of C-H and C-F bonds in α -phase at 763, 769, 976, 1149 and 1210 cm^{-1} and the appearance of new exclusive absorption signals at 840 cm^{-1} attributed to the β -phase. Whilst, the γ -phase and mutually co-existing β - and γ -phases of PVDF remains unaffected.

3.2. Evidences from the Raman spectroscopy

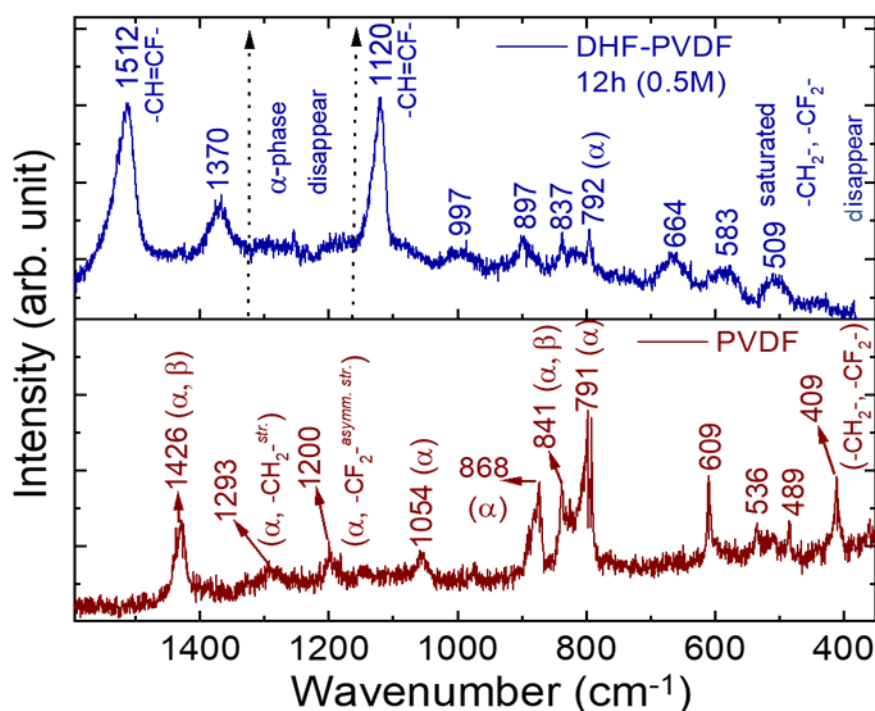


Fig 2. Raman spectra of PVDF (bottom) and dehydrofluorinated PVDF (upper) in the expansion range of \square 1600 cm^{-1} - 350 cm^{-1} after treating with 0.5 M NaOH for 12 h at $25\text{ }^{\circ}\text{C} \pm 1\text{ }^{\circ}\text{C}$.

The Raman spectra of PVDF and dehydrofluorinated PVDF were obtained to confirm complementary vibrational modes for various phases and mutually exclusive shifts, which are IR inactive but strongly Raman active, especially the near centrosymmetric double bonds. **Figure 2** illustrates the comparative Raman spectra of PVDF and the dehydrofluorinated polymer. It is evident that after the dehydrofluorination reaction, peaks undergo considerable shift and display new modes of vibration between 1595 cm^{-1} and 350 cm^{-1} . In PVDF, the band at 409 cm^{-1} is assigned to rocking mode of vibration (for mutually co-existing $-\text{CF}_2-$ and $-\text{CH}_2-$ groups) [49, 50]. Whilst, the peak at 489 cm^{-1} is attributed to the stretching/wagging vibrations (for $-\text{CF}_2-$ group). Moreover, the rocking bending modes in the α -phase at 791 cm^{-1} is characteristic of the methylene ($-\text{CH}_2-$) groups in PVDF. At 841 cm^{-1} , the co-existence of the α - and β -phases for the combined overlap of $-\text{CH}_2-$ rocking and asymmetric stretching of $-\text{CF}_2-$ is also observed. The carbon skeleton and its various vibrations were identified at 868 cm^{-1} and 1054 cm^{-1} for C-C symmetric stretching with C-C-C scissoring vibrations and C-C asymmetric stretching with $-\text{CH}_2-$ wagging for the α -phase, respectively [49]. Furthermore, in PVDF, the region between 850 cm^{-1} and 1500 cm^{-1} is critically important to understand the dehydrofluorination reaction with respect to the involvement of reactive phases and the change in bonding attributes. For instance, in PVDF, the asymmetric stretching and bending modes of vibration for $-\text{CF}_2-$ and $-\text{CH}_2-$ (wagging) in the α -phases were assigned at 1200 cm^{-1} and 1293 cm^{-1} . In addition, the sharp and intense Raman shift at 1426 cm^{-1} corresponds to the $-\text{CH}_2-$ bending vibration mode in mixed phase viz the α - and β -phases which plausibly acquired the modified orientation in alkali treated PVDF. Moreover, it is observed that the functional transformation affects the vibration modes of $-\text{CH}_2-$, $-\text{CF}_2-$, C-C and C-C-C in PVDF skeleton. Thus, the comparison on consumed bonds and newly acquired groups in dehydrofluorinated PVDF was corroborated [51]. It illustrates the comprehensive information on the most reactive phase of PVDF during dehydrofluorination reaction in alkaline media [52]. In

dehydrofluorinated PVDF, the Raman active vibration at 509 cm^{-1} , 583 cm^{-1} and 664 cm^{-1} correspond to different C-C bonding and the shifts are attributed to the changes acquired in the polymer chain conformation due to olefin bonds. Evidently, the peaks at the 1054 cm^{-1} , 1200 cm^{-1} , 1293 cm^{-1} and 1426 cm^{-1} for the α -phases of methylene and difluoromethylene motifs completely disappears in dehydrofluorinated PVDF and very prominent peaks are observed at 1120 cm^{-1} , 1370 cm^{-1} and 1512 cm^{-1} for the olefin -CH=CF- vibration of polyenes suggesting that the dehydrofluorination occurs [45]. In addition, the wagging and stretching vibrations for -CF₂- and -CH₂- between region 1200 cm^{-1} to 1300 cm^{-1} tend to reduce confirming the consumption of F- and H-atoms, respectively. The retention in peak at 837 cm^{-1} signifies that the mixed β - and γ -phases do not considerably change (a shoulder peak is observed in the spectrum of PVDF). These results supplement the observations made using ATR-IR spectroscopy. Thus, based on the results, the α -phase predominately reacts over other phases in PVDF during the dehydrofluorination reaction.

3.3. Evidences from NMR spectroscopy and mechanisms

Twum et al. [36] comprehensively characterized the chemical structure of PVDF by ¹H, ¹³C and ¹⁹F NMR spectroscopy. Results signifies that the intrinsic chemical and physical property of macromolecules relates to the orientation of bond and can help in understanding the polymerization reaction. Hence, it is important to acquire better and comprehensive understanding of polymer structures [36]. **Figure 3** illustrates the time resolved high resolution ¹H-NMR spectra of PVDF when treated with low alkali concentration (i.e., 0.5 M NaOH) to get dehydrofluorinated PVDF at intervals of 4 h, 8 h and 24 h, respectively.

Assigning the functional transformation in head-to-tail region: In the ¹H-NMR of PVDF (**Figure 3**), the two orientations viz the head-to-tail (-CH₂CF₂-CH₂-CF₂-) and tail-to-tail (-CF₂CH₂-CH₂-CF₂-) are prominently evident at δ 2.97 ppm (multiplet, 2H) and δ 2.37 ppm (triplet, 2H), respectively. Moreover, the PVDF consists mainly of head-to-tail orientation with δ 95 %-97 % proportion [37]. The peaks ranging from δ 1.0 ppm to 1.85 ppm and at 6.32 ppm is attributed due to the methane radical tail and branching with capping terminal groups, respectively [53]. In previous reports [54-

56], after the dehydrofluorination of PVDF and VDF co-polymers, the peak between 5.5 ppm to 6.0 ppm is assigned to the formation of double bond. However, to the best of our knowledge, the fingerprint region (here, the 3.25 ppm to 2.15 ppm) of the products are not elucidated in detailed manner. Referring to the study by Zhang et al. [57], the dehydrofluorination of poly(VDF-co-TrFE) copolymer occurs at tail-to-tail region of fluorinated co-polymer where the influence of -I-effect of difluoromethylene units was probably remained unclear. Whilst, Ahmed et al. [15, 26] confers in mechanism that the dehydrofluorination of PVDF in NaOH/propan-2-ol proceeds through six membered transition state with a hydrogen transfer step from propan-2-ol to PVDF backbone (as hydride, from mechanism), generating acetone (confirmed from experimental detection) [15]. Moreover, in the dehydrofluorination studies of poly(VDF-*ter*-HFP-*ter*-TFE) and poly(VDF-co-HFP) copolymers, the deconvolutions of 2.8 ppm to 3.2 ppm region in the spectrum were limited to low field shifts (viz the olefin region). The subtle yet decisive splitting in the peak near 3.2 ppm regions of dehydrofluorinated poly(VDF-co-HFP) copolymer were also required to be comprehensively discussed. Interestingly, the unsaturation induces changes in 2.8 ppm to \square 3.2 ppm region of NMR spectrum and was assigned to the $-\text{CH}_2\text{CF}_2^{\text{h}}\text{CH}_2^{\text{t}}\text{CF}_2-$ of DHF-PVDF. Progressively with time, the new peak close to 3.02 ppm is attributed to the methylene group adjacent to the vinylic proton ($-\text{CH}_2\text{CF}=\text{CH}-$) of DHF-PVDF (inset highlighted). Whilst, the peak for $-\text{CF}_2\text{CH}_2^{\text{h}}\text{CH}_2^{\text{t}}\text{CF}_2-$ orientation remains unchanged showing that the reaction is not occurring at the tail-to-tail functional orientation (**Figure 3** in the \square 2.4 ppm region). These results are decisive and justify the prominent reactive site in PVDF during dehydrofluorination reaction. Also, based on the ^1H -NMR results, we infer that the reaction of dehydrofluorination is head-to-tail selective and plausibly proceeds rapidly when the H- and F-atoms are in *anti*-periplanar where both H- and F-atoms are in anti-axial (180°) positions in comparison to *syn*-periplanar conformation where both H- and F-atoms are in syn-axial positions (0°) (**Scheme 2**). Since, the former is thermodynamically more stable form over the *cis*-configuration, we also elucidated that the dehydrofluorination can be mediated by *in-situ* generated sodium iso-propoxide as reported by Ahmed et al. [15, 26] and simultaneously it can be catalyzed by the free hydroxides present in the system.

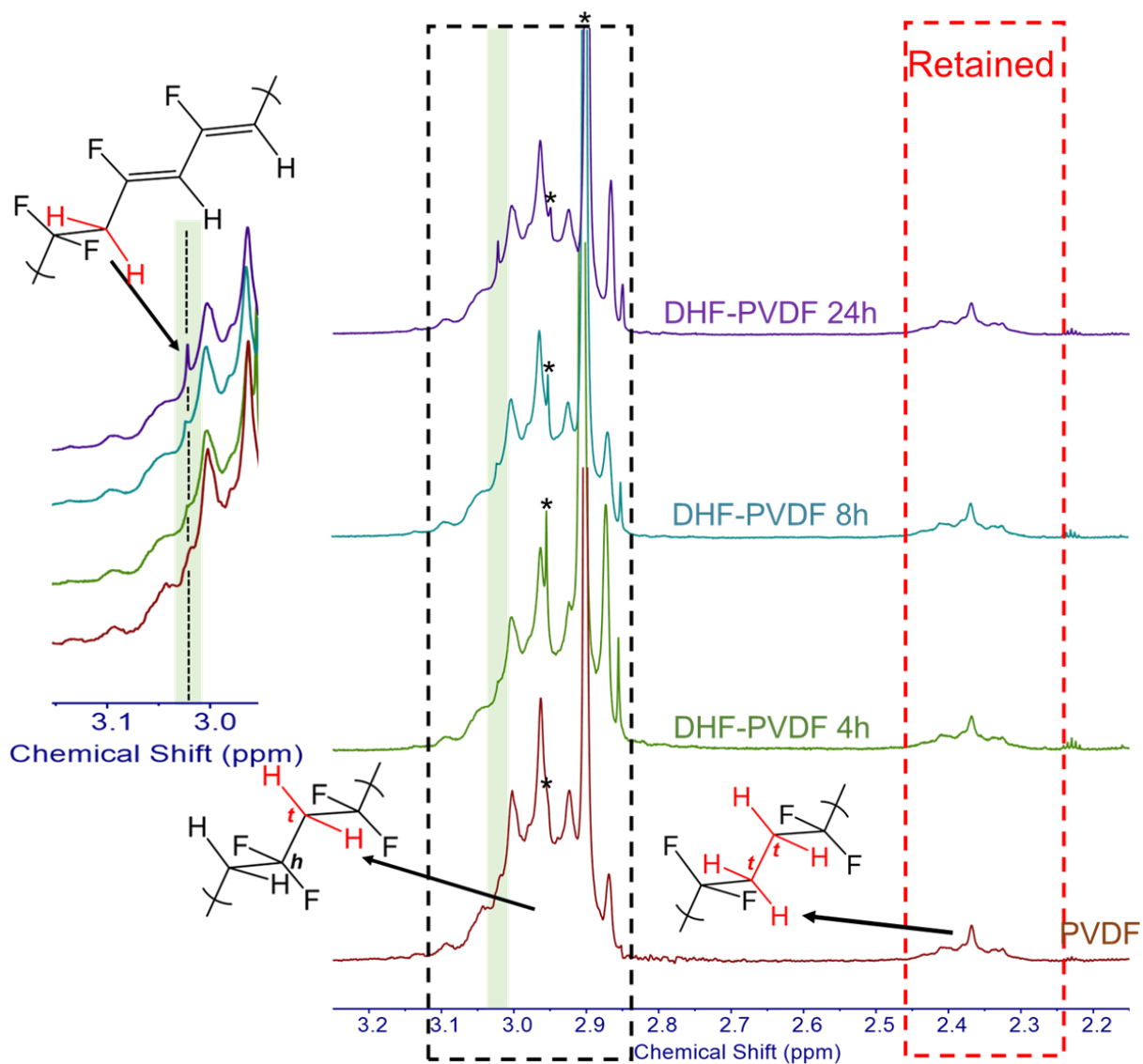
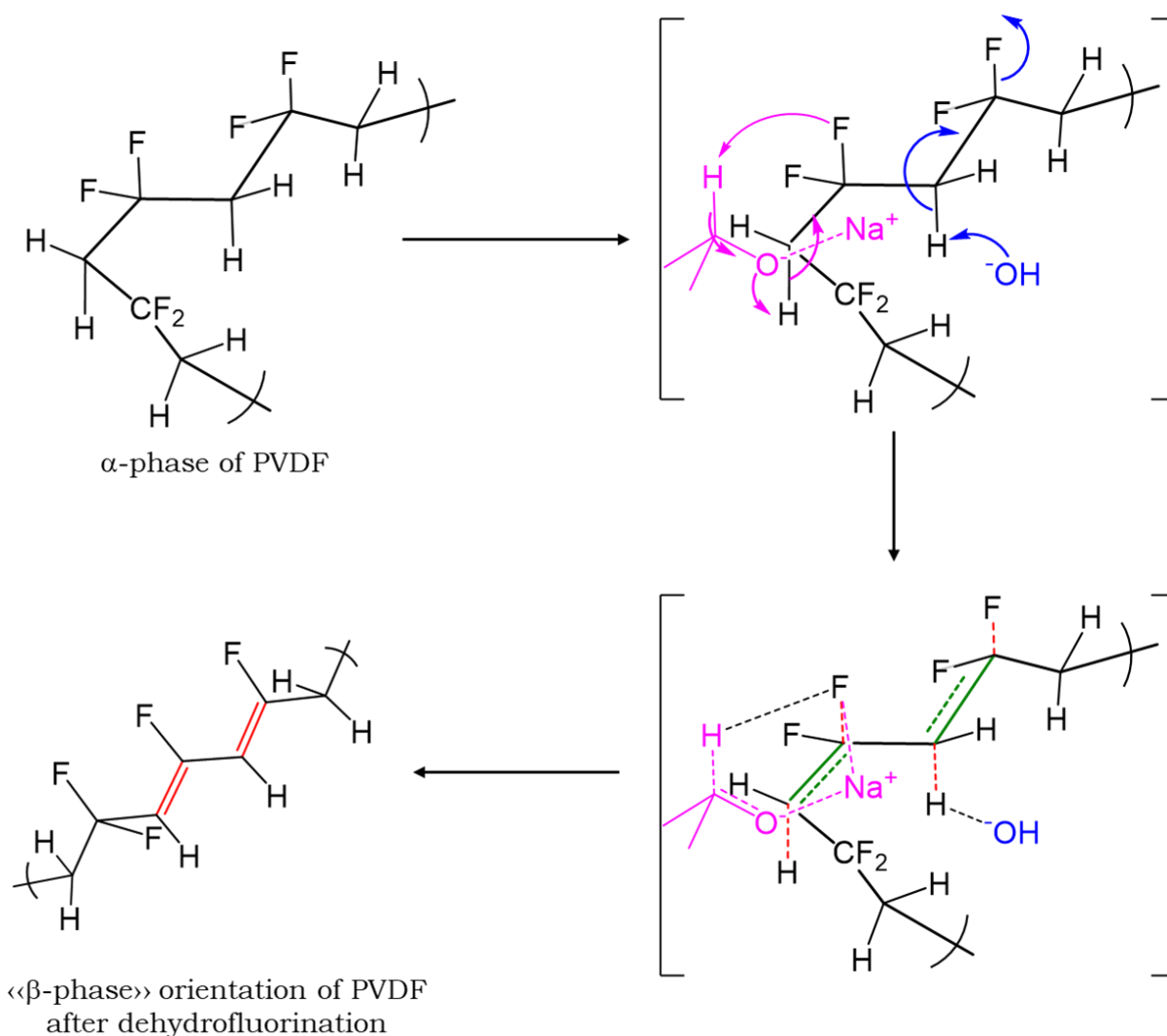


Figure 3. Expansion of the 2.2 to 3.25 ppm zone of the ^1H -NMR spectra of the PVDF (bottom) and dehydrofluorinated PVDF in acetone- d_6 and obtained at different times using sodium hydroxide (0.5 M NaOH) and propan-2-ol defining the site reactivity of head-to-tail (H-T) over tail-to-tail (T-T) orientation.

To understand the mechanism, both sodium iso-propoxide and sodium hydroxide afford the dehydrofluorination of PVDF. The following steps are proposed for such a reaction (**Scheme 2**):

- i.)** The activation of propan-2-ol to generate non-nucleophilic iso-propoxide base for H-abstraction,
- ii.)** Proton abstraction from the contorted polymer network of PVDF from anti-periplanar or syn-periplanar manner via the bimolecular elimination (E_2) reaction route and pushing the F-atom in six membered cyclic transition state and,

iii.) HF elimination by proton abstraction from iso-propoxide in concerted manner.



Scheme 2. Proposed mechanism of dehydrofluorination in head-to-tail site of PVDF in solution phase (favourable conformation for dehydrofluorination: anti-periplanar arrangement of H- and F-atom).

Evidences of disappearance of double bond due to hydroxide attack: As evident in spectrum (**Figure 4**), the two sets of olefinic protons are visualized as distorted broad complex multiplet at 5.4 ppm and 6.1 ppm attributed to the $-(\text{CH}_2-\text{CH}=\text{CF}-\text{CH}_2-\text{CF}_2)-$ and $-(\text{CF}_2-\text{CH}=\text{CF}-\text{CH}_2-\text{CF}_2)-$, respectively. Moreover, attributed to high reactivity of these double bonds and due to the presence of F-atoms and $-\text{CF}_2-$ unit, the unsaturated sites can be attacked by hydroxides to form the corresponding oxidized PVDF [12, 58]. Depending upon the dehydrofluorination reagent viz the

alkali base, amines, metal hydrides, etc., the mechanism vary from elimination reactions (viz E₁, E₂ or β-H elimination) to single electron transfer. On evaluating the olefin region (5.0 ppm to 6.0 ppm) of the ¹H-NMR spectra, result suggests that the olefin proton in dehydrofluorinated PVDF first appears for initial hours (up to 12 h) and then disappears showing that the prolonged reaction (≥ 14 h) can reduce the scope for further functional modifications attributed to the loss of unsaturation (i.e., vanishing of the signal centred at 5.4 ppm, **Figure 4**).

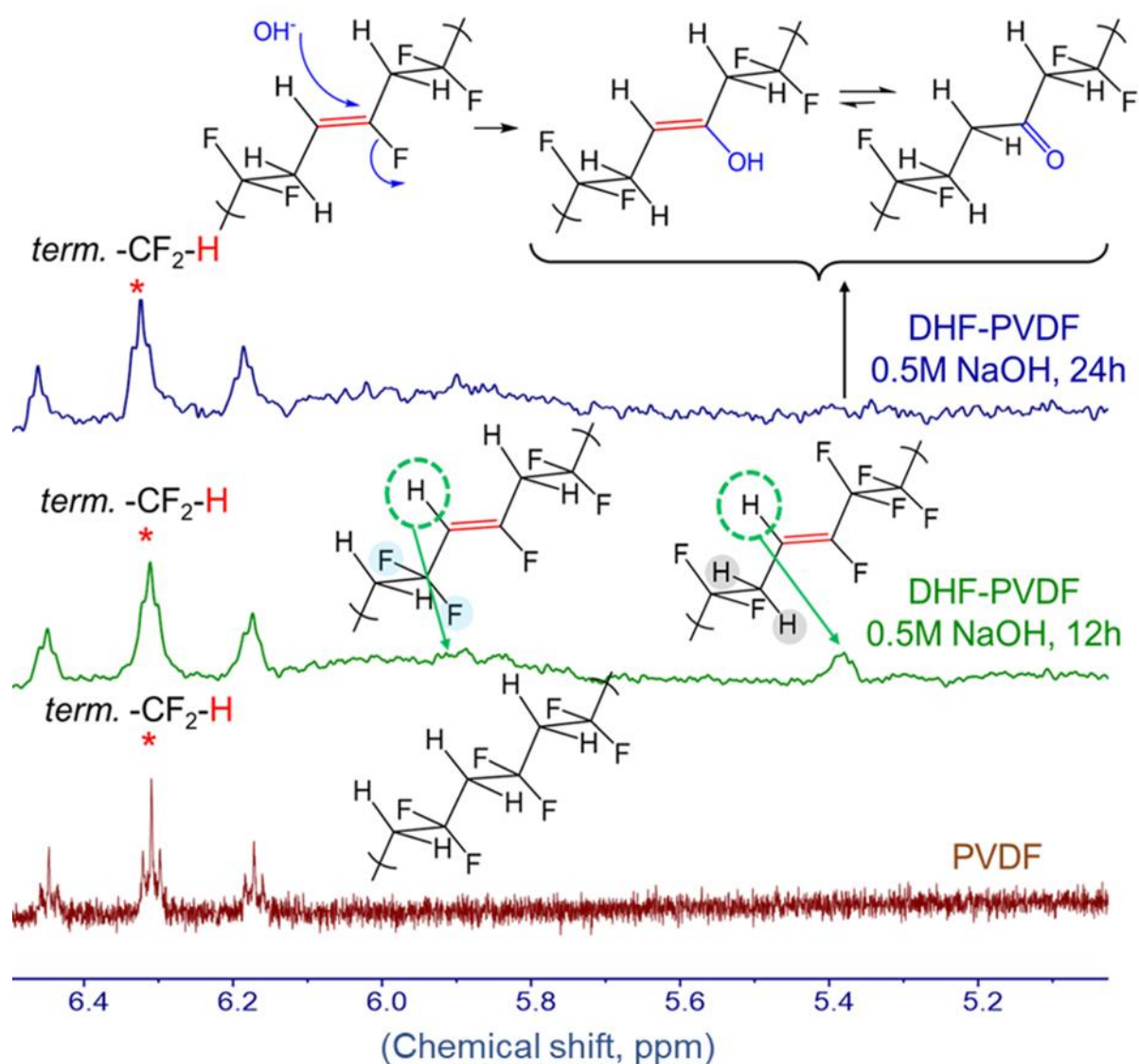
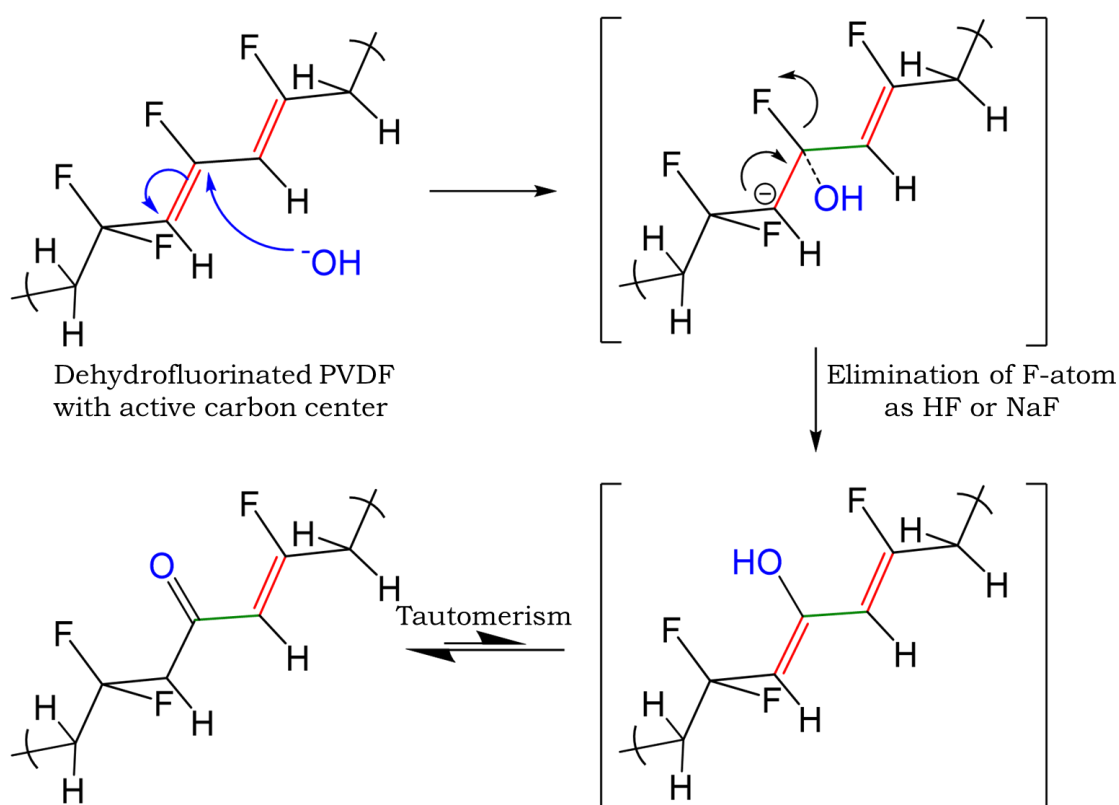


Figure 4. Expansion of the 5.0 to 6.5 ppm zone from the ¹H-NMR spectra of PVDF (bottom) and dehydrofluorinated PVDF (middle and upper) in Acetone-d₆ at different times using sodium hydroxide (0.5 M NaOH) and propan-2-ol.

Furthermore, to investigate the hydroxide attack over the sp^2 C-atom of dehydrofluorinated PVDF and its oxidation the region of 2.8 ppm to 3.0 ppm reveals several peaks. Meanwhile, the high-resolution spectra of unsaturated PVDF and PVDF, show that the peak at \square 2.88 ppm in PVDF disappears while a new broad singlet shielded at \square 2.82 ppm is observed (**Figure S1**), attributed to the oxidized keto form of the PVDF. These results strongly affirm the functional interconversions of DHF-PVDF into the oxidised forms as mentioned in previous literature [55].

The mechanism for oxidation step during prolonged dehydrofluorination ($t > 12-14$ h) plausibly follows the order (**Scheme 3**):

- i.)** The nucleophilic attack of hydroxide onto the sp^2 -carbon atom forming a fluoro-hydroxyl tetrahedral system with carbanion at adjacent carbon,
- ii.)** Delocalization of formed carbanion to eliminate the F-atom and to form enol-system and,
- iii.)** Transformation of enol to keto form through keto-enol tautomerism.



Scheme 3. Possible mechanism for the oxidation of dehydrofluorinated PVDF backbone under the influence of prolonged alkali treatments.

Crosslinking in the contorted network occurs through backbiting: Crosslinking in PVDF based polymers generally proceeds through tailoring of the nucleophilic moieties for instance bis-amines, bis-phenates and cross linkers [18, 28, 29, 59, 60]. However, with higher dehydrofluorination time the partial internal crosslinking within alkaline conditions were evident (**Scheme 4, Figure S2**). PVDF bearing appreciably acidic proton, is susceptible to the elimination of proton and the formed carbanions backbites the contorted polymer chain with simultaneous removal of HF from the system. Attributed to difference in s-character of the aliphatic and cyclic crosslinked olefin proton, the proton reflects different shifts in NMR spectrum. To consolidate the solid difference, it was worth obtaining ^1H -NMR and ^1H $\{^{19}\text{F}\}$ -NMR spectra in 5.0 to 6.5 ppm region showing two different sets of protons (**Figure 5**). For the partial internal crosslinking of PVDF in alkaline medium, the plausible order is as follows (**Scheme 4**):

- i.)** Abstraction of proton by the hydroxide ion from the PVDF backbone to form carbanion,
- ii.)** And, the [1,6]-nucleophilic attack of the formed carbanion to form cyclic system with internal crosslinking in PVDF polymer (since, the reaction proceeds via anion intermediate, and called “*carbanion backbiting*”).

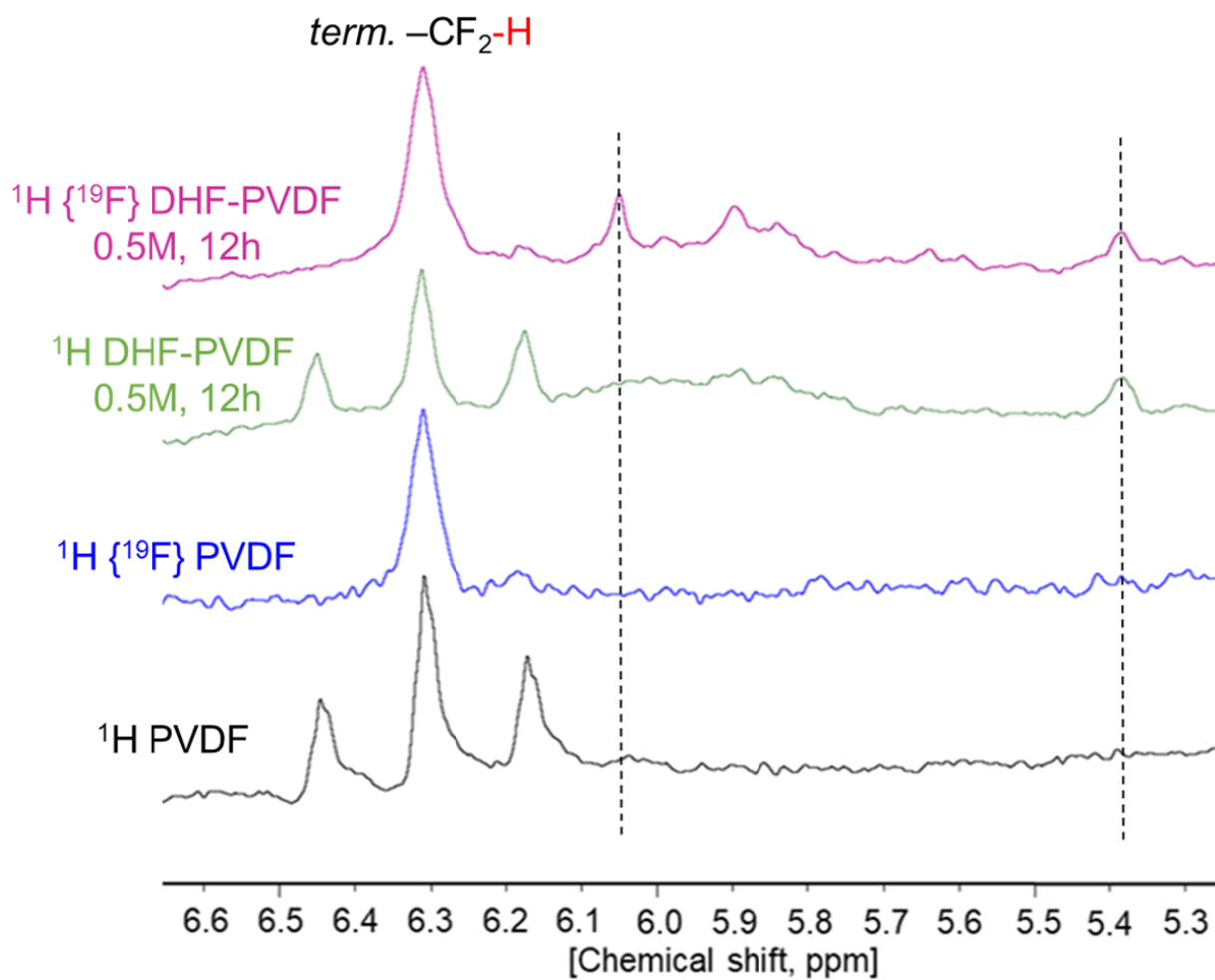
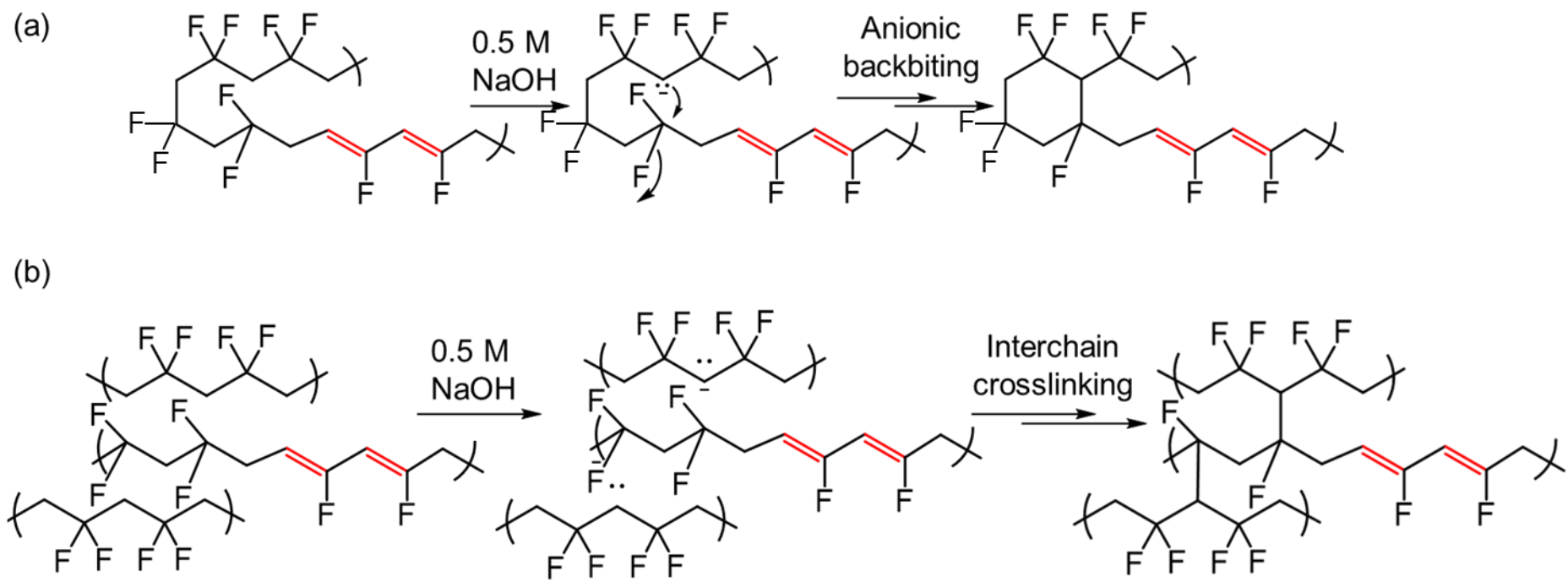


Figure 5. $^1\text{H } \{^{19}\text{F}\}$ -NMR spectra in olefin region in dehydrofluorinated PVDF in Acetone- d_6 (Extended from Figure 4. at 4.0 level of line broadening to remove any discrete noise in signals using TopSpin 4.1.4 application).



Scheme 4. Possible mechanism for partial crosslinking with simultaneous dehydrofluorination when performed for long reaction time with high alkali concentration: (a) crosslinking via carbanion backbiting via the pull-push mechanism and (b) interchain crosslinking .

Acquisition of heteronuclear correlation spectra and evidences on unsaturated ^1H and ^{19}F - nuclei correlation: In the above discussion, the 1D ^1H -NMR spectroscopic analysis were used to probe the reaction sites and understand the mechanism for dehydrofluorination reaction. Furthermore, to acquire the evidences on unsaturation sites induced in PVDF, the relationship between the ^1H and ^{19}F nuclei was corroborated using 2D heteronuclear correlation spectroscopy (hetero COSY) analysis (**Figure 6**). Region I with variable sets of ^1H - ^{19}F correlation of the spectrum shows peak for possible tail-to-tail and head-to-tail heteronuclear correlations. The correlation contour in the Region II confirms that the F- and H-atoms on the double bond mutually correlates at the δ 6.0 ppm ($-\text{CH}=\text{}$) and δ -119.5 ppm ($=\text{CF}-$). Hence this unprecedented 2D NMR junction ($x^1\text{H}$, $y^{19}\text{F}$ = 6.0, -119.5) strongly confers the existence of $-\text{CH}=\text{CF}-$ unit in dehydrofluorinated PVDF (**Figures S3 and S4**).

Conclusion

The scope of this study underlies describing the chemical transformation (especially, the unsaturated site formation) in PVDF when treated with sodium hydroxide/propan-2-ol. The transformations in different phases and the orientations of PVDF during the dehydrofluorination reaction is investigated. The dehydrofluorination reaction was evidenced by infrared, Raman and nuclear magnetic resonance spectroscopies (^1H and $1\text{H}\{^{19}\text{F}\}$) in detailed manner and plausible mechanistic insights for dehydrofluorination of PVDF is presented. Infrared spectroscopy suggests strong correlation between the consumption of C-H and C-F bonds of PVDF from the α -phase and evolution of exclusive absorption signals for the β -phase. Moreover, due to centrosymmetric attributes of the olefinic bond, the signal at 1624 cm^{-1} was further studied by Raman spectroscopy. Results suggests that the unsaturation sites in dehydrofluorinated PVDF can be understood more clearly by observing sharp vibration bands at 1120 , 1370 and 1512 cm^{-1} . In addition, the correlation between various phases is discussed. Investigation of NMR spectra reveals that the dehydrofluorination is site selective and the double bond formation is more pronounced at head-to-tail ($-\text{CH}_2^t\text{CF}_2^h-$) orientation whilst, the tail-to-tail ($-\text{CH}_2^t\text{CH}_2^t-$) methylene-difluoromethylene groups remain unaffected. However, the estimation of the number of double bonds cannot be supplied, as well as the isolated or conjugated ones. The crosslinking mechanism at higher alkaline concentrations is described by “carbanion backbiting” phenomena.

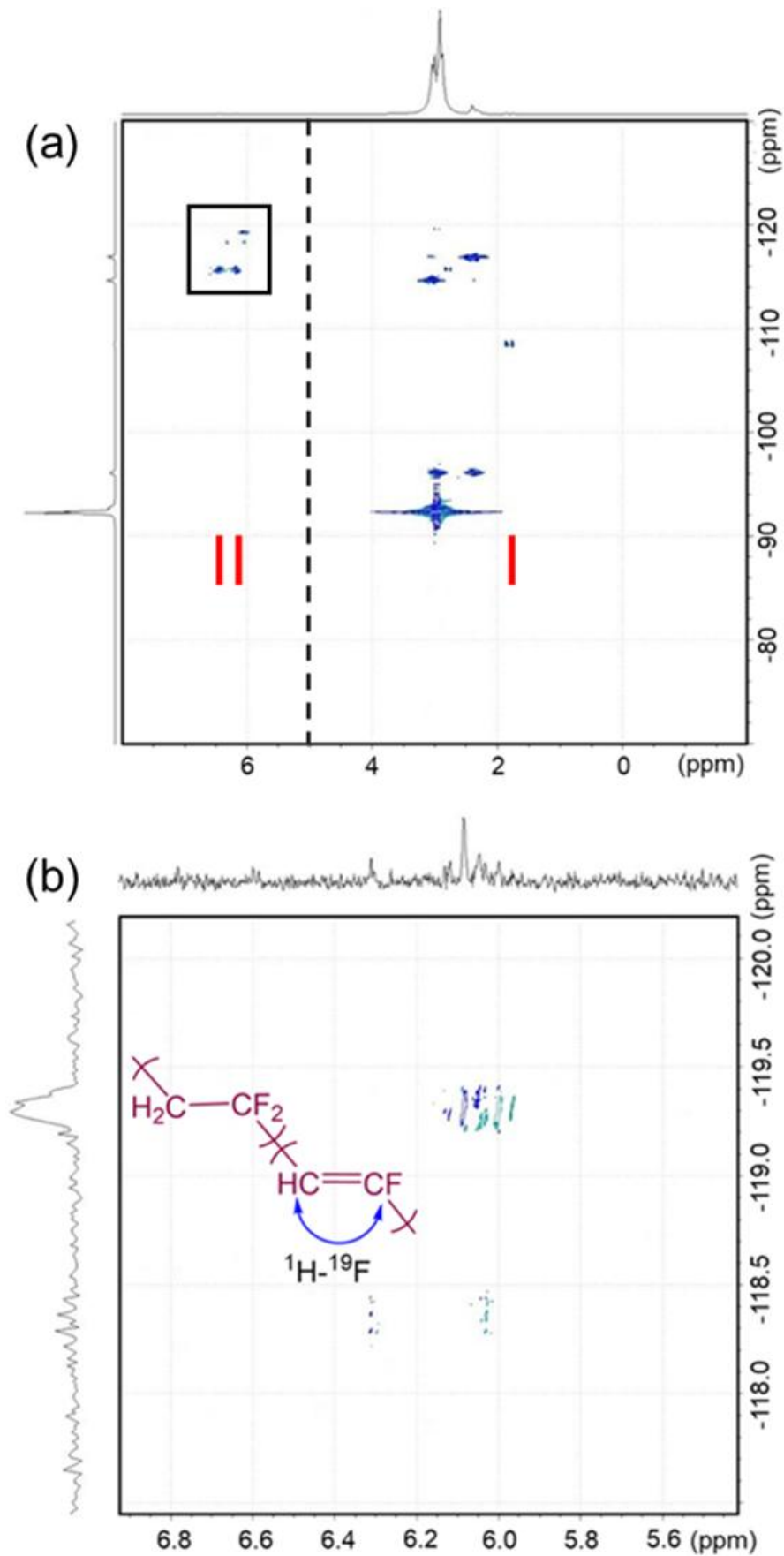


Figure 6. 2D ^1H - ^{19}F HETCOR spectra of dehydrofluorinated PVDF (a) full spectra and (b) the expansion showing the correlation of $-\text{CH}=\text{CF}-$ olefin moieties (sample prepared in Acetone- d_6).

We also validate the hydroxyl attack onto the activated fluorinated-olefinic carbon (analogous to sp^2 -C akin carbonyl) which is evident by the vanishing of peak in \square 5.4 ppm region of ^1H -NMR spectrum. The olefinic functionality $-(\text{CH}=\text{CF})-$ and the existence of prominent trans-configuration of $-(\text{CH}^t=\text{CF}^h)-$ is evidenced by IR spectroscopy. Furthermore, the dehydrofluorination was supplemented by the novel ^1H and ^{19}F correlation spectroscopy (hetero COSY) and the junction at the ($x^{1\text{H}}, y^{19\text{F}} = 6.0, -119.5$) inevitably confirms the formation of $-(\text{CH}=\text{CF})-$ double bond. To conclude, **this unprecedented report clearly evidences the dehydrofluorination on the specific site of PVDF and proposes features to understand the detailed chemistry of dehydrofluorination of PVDF** and related niche fluoropolymers for future studies.

Acknowledgements

B. A. acknowledges French fluorine network (GIS Fluor) and PEPR (ANR-22-PERE-0008), V. K. thanks grant number: MLP 0076 (CSIR-CSMCRI funded project) and J. S acknowledges the financial support to Indo-French Centre for the Promotion of Advanced Research (IFCPAR/CEFIPRA), University Grant Commission (UGC, File No. 191620048179) and French National Center for Scientific Research (CNRS) for the financial and laboratory support under the Raman-Charpak Fellowship (RCF) program [OM offer no.: IFC//4141/RCF 2022/375].

Conflict of Interest

The authors declare that they have no known competing financial interests or personal relationships that could have appeared to influence the work reported in this manuscript.

References

1. A. D. Asandei, Photomediated Controlled Radical Polymerization and Block Copolymerization of Vinylidene Fluoride. *Chem. Rev.* 2016, 116 (4), 2244-2274. <https://doi.org/10.1021/acs.chemrev.5b00539>
2. J. T. Goldbach, R. Amin-Sanayei, W. He, J. Henry, W. Kosar, A. Lefebvre, G. O'Brien, D. Vaessen, K. Wood, S. Zerafati, Commercial Synthesis and Applications of Poly (Vinylidene Fluoride). *Fluorinated Polymers* 2016, 2, 127-157.
3. F. Mammeri, Chapter 3 - Nanostructured Flexible PVDF and Fluoropolymer-Based Hybrid Films. *In Frontiers of Nanoscience*, Benelmekki, M.; Erbe, A., Eds. Elsevier: 2019; Vol. 14, pp 67-101.

- 4.** R. Dallaev, T. Pisarenko, D. Sobola, F. Orudzhev, S. Ramazanov, T. Trčka, Brief Review of PVDF Properties and Applications Potential *Polymers* 2022, 14 (22), 4793. <https://doi.org/10.3390/polym14224793>
- 5.** B. Ameduri, Fluoropolymers: A Special Class of Per- and Polyfluoroalkyl Substances (PFASs) Essential for Our Daily Life. *J. Fluor. Chem.* 2023, 267, 110117. <https://doi.org/10.1016/j.jfluchem.2023.110117>
- 6.** G. J. Puts, P. Crouse, B. Ameduri, Polytetrafluoroethylene: Synthesis and Characterization of the Original Extreme Polymer. *Chem. Rev.* 2019, 119 (3), 1763-1805. <https://doi.org/10.1021/acs.chemrev.8b00458>
- 7.** B. Ameduri, From Vinylidene Fluoride (VDF) to the Applications of VDF-Containing Polymers and Copolymers: Recent Developments and Future Trends. *Chem. Rev.* 2009, 109 (12), 6632-6686. <https://doi.org/10.1021/cr800187m>
- 8.** J. Hamaura, R. Honma, H. Hori, A. Manseri, B. Ameduri, Efficient fluoride recovery from poly(vinylidene fluoride), poly(vinylidene fluoride-co-hexafluoropropylene) copolymer and poly(ethylene-co-tetrafluoroethylene) copolymer using superheated water with alkaline reagent. *Euro. Polym. J.* **2023**, 182, 111724. <https://doi.org/10.1016/j.eurpolymj.2022.111724>
- 9.** P. Saxena, P. Shukla, A Comprehensive Review on Fundamental Properties and Applications of Poly(Vinylidene Fluoride) (PVDF). *Adv. Compos. Hybrid Mater.* 2021, 4 (1), 8-26. <https://doi.org/10.1007/s42114-021-00217-0>
- 10.** S. Varun, N. M. George, A. M. Chandran, L. A. Varghese, P. K. S. Mural, Multifaceted PVDF Nanofibers in Energy, Water and Sensors: A Contemporary Review (2018 to 2022) and Future Perspective. *J. Fluor. Chem.* 2023, 265, 110064. <https://doi.org/10.1016/j.jfluchem.2022.110064>
- 11.** H. Kise, H. Ogata, Phase Transfer Catalysis in Dehydrofluorination of Poly(Vinylidene Fluoride) by Aqueous Sodium Hydroxide Solutions. *J. Polym. Sci.* 1983, 21 (12), 3443-3451. <https://doi.org/10.1002/pol.1983.170211208>.
- 12.** G. J. Ross, J. F. Watts, M. P. Hill, P. Morrissey, Surface Modification of Poly(Vinylidene Fluoride) by Alkaline Treatment 1: The Degradation Mechanism. *Polymer* 2000, 41 (5), 1685-1696. [https://doi.org/10.1016/S0032-3861\(99\)00343-2](https://doi.org/10.1016/S0032-3861(99)00343-2).
- 13.** T. N. Danks, R. C. T. Slade, J. R. Varcoe, Alkaline Anion-Exchange Radiation-Grafted Membranes for Possible Electrochemical Application in Fuel Cells. *J. Mater. Chem.* 2003, 13 (4), 712-721. <https://doi.org/10.1039/B212164F>.

- 14.** G. Couture, A. Alaaeddine, F. Boschet, B. Ameduri, Polymeric Materials as Anion-Exchange Membranes for Alkaline Fuel Cells. *Prog. Polym. Sci.* 2011, 36 (11), 1521-1557. <https://doi.org/10.1016/j.progpolymsci.2011.04.004>.
- 15.** M. M. Ahmed, J. Hrůza, M. Stuchlík, V. Antoř, J. Müllerová, M. Řezanka, Revisiting the Polyvinylidene Fluoride Heterogeneous Alkaline Reaction Mechanism in Propan-2-ol: An Additional Hydrogenation Step. *Eur. Polym. J.* 2021, 156, 110605. <https://doi.org/10.1016/j.eurpolymj.2021.110605>.
- 16.** K. Feng, B. Tang, P. Wu, Ammonia-Assisted Dehydrofluorination between PvdF and Nafion for Highly Selective and Low-Cost Proton Exchange Membranes: A Possible Way to Further Strengthen the Commercialization of Nafion. *J. Mater. Chem. A* 2015, 3 (24), 12609-12615. <https://doi.org/10.1039/C5TA02855H>.
- 17.** Y. Wang, H. Wang, K. Liu, T. Wang, C. Yuan, H. Yang, Effect of Dehydrofluorination Reaction on Structure and Properties of PVDF Electrospun Fibers. *RSC Adv.* 2021, 11 (49), 30734-30743. <https://doi.org/10.1039/D1RA05667K>.
- 18.** J. Sierke, A. V. Ellis, Cross-Linking of Dehydrofluorinated PVDF Membranes with Thiol Modified Polyhedral Oligomeric Silsesquioxane (POSS) and Pure Water Flux Analysis. *J. Membr. Sci.* 2019, 581, 362-372. <https://doi.org/10.1016/j.memsci.2019.03.063>.
- 19.** S. Owusu-Nkwantabisah, M. Robbins, D. Y. Wang, Towards Superhydrophobic Coatings Via Thiol-Ene Post-Modification of Polymeric Submicron Particles. *Appl. Surf. Sci.* 2018, 450, 164-169. <https://doi.org/10.1016/j.apsusc.2018.04.182>.
- 20.** M.-K. Song, Y.-T. Kim, J. M. Fenton, H. R. Kunz, H.-W. Rhee, Chemically-Modified Nafion®/Poly(Vinylidene Fluoride) Blend Ionomers for Proton Exchange Membrane Fuel Cells. *J. Power Sources* 2003, 117 (1), 14-21. [https://doi.org/10.1016/S0378-7753\(03\)00166-6](https://doi.org/10.1016/S0378-7753(03)00166-6).
- 21.** A. Rajput, J. Sharma, S. K. Raj, V. Kulshrestha, Dehydrofluorinated Poly(Vinylidene Fluoride-co-Hexafluoropropylene) Based Crosslinked Cation Exchange Membrane for Brackish Water Desalination Via Electrodialysis. *Colloids Surf. A: Physicochem. Eng.* 2021, 630, 127576. <https://doi.org/10.1016/j.colsurfa.2021.127576>.
- 22.** J. Castillo, A. Robles-Fernandez, R. Cid, J. A. González-Marcos, M. Armand, D. Carriazo, H. Zhang, A. Santiago, Dehydrofluorination Process of Poly (Vinylidene Difluoride) PVDF-Based Gel Polymer Electrolytes and Its Effect on Lithium-Sulfur Batteries. *Gels* 2023, 9 (4), 336. <https://doi.org/10.3390/gels9040336>

- 23.** A. Taguet, L. Sauguet, B. Ameduri, B. Boutevin, Fluorinated Cotelomers Based on Vinylidene Fluoride (VDF) and Hexafluoropropene (HFP): Synthesis, Dehydrofluorination and Grafting by Amine Containing an Aromatic Ring. *J. Fluor. Chem.* 2007, 128 (6), 619-630. <https://doi.org/10.1016/j.jfluchem.2007.02.005>.
- 24.** A. Taguet, B. Ameduri, A. Dufresne, Crosslinking and Characterization of Commercially Available Poly(VDF-co-HFP) Copolymers with 2,4,4-Trimethyl-1,6-Hexanediamine. *Eur. Polym. J.* 2006, 42 (10), 2549-2561. <https://doi.org/10.1016/j.eurpolymj.2006.04.012>.
- 25.** W. Zhu, K. Okada, N. Hoshida, Y. Yoshida, A. Martucci, J. Zhu, E. Marin, G. Pezzotti, Effect of Carbonate Source on the Dehydrofluorination Process in Polyvinylidene Fluoride/Alkali Metal Carbonate Composites. *ACS Omega* 2023, 8 (17), 14944-14951. <https://doi.org/10.1021/acsomega.2c06857>.
- 26.** M. M. Ahmed, J. Hrůza, M. Stuchlík, V. Antoš, J. Müllerová, M. Řezanka, Corrigendum to “Revisiting the Polyvinylidene Fluoride Heterogeneous Alkaline Reaction Mechanism in Propan-2-ol: An Additional Hydrogenation Step” [*Eur. Polym. J.* 156 (2021) 110605]. *Eur. Polym. J.* 2021, 159, 110710. <https://doi.org/10.1016/j.eurpolymj.2021.110710>.
- 27.** S. Zulfiqar, M. Zulfiqar, M. Rizvi, A. Munir, I. C. McNeill, Study of the Thermal Degradation of Polychlorotrifluoroethylene, Poly(Vinylidene Fluoride) and Copolymers of Chlorotrifluoroethylene and Vinylidene Fluoride. *Polym. Degrad. Stab.* 1994, 43 (3), 423-430. [https://doi.org/10.1016/0141-3910\(94\)90015-9](https://doi.org/10.1016/0141-3910(94)90015-9).
- 28.** W. W. Schmiegel, Crosslinking of Elastomeric Vinylidene Fluoride Copolymers with Nucleophiles. *Die Angewandte Makromolekulare Chemie* 1979, 76 (1), 39-65. <https://doi.org/10.1002/apmc.1979.050760103>.
- 29.** A. Taguet, B. Ameduri, B. Boutevin, Crosslinking of Vinylidene Fluoride-Containing Fluoropolymers. In *Crosslinking in Materials Science*, Springer Berlin Heidelberg: Berlin, Heidelberg, 2005; pp 127-211.
- 30.** K. H. Girish, P. V. Sainnath, P. B. Rasoor, P. B. Structure–Property Study of Pristine and Dehydrofluorinated Poly(Vinylidene Fluoride) Using Density Functional Theory. *Monatshefte für Chemie - Chemical Monthly* 2021, 152 (5), 559-567. <https://doi.org/10.1007/s00706-021-02766-y>.
- 31.** L. Cozzarini, C. Schmid, Failure of Fluorocarbon Copolymer Pipes Subjected to Mechanical Strain in an Alkaline Environment. *Eng. Fail. Anal.* 2021, 128, 105572. <https://doi.org/10.1016/j.engfailanal.2021.105572>.
- 32.** S. Tan, J. Li, G. Gao, H. Li, Z. Zhang, Synthesis of Fluoropolymer Containing Tunable Unsaturation by a Controlled Dehydrochlorination of P(VDF-co-CTFE) and

Its Curing for High Performance Rubber Applications. *J. Mater. Chem.* 2012, 22 (35), 18496-18504. <https://doi.org/10.1039/C2JM33133K>.

33. D. Li, M. Liao, Dehydrofluorination Mechanism, Structure and Thermal Stability of Pure Fluoroelastomer (Poly(VDF-*ter*-HFP-*ter*-TFE) Terpolymer) in Alkaline Environment. *J. Fluor. Chem.* 2017, 201, 55-67. <https://doi.org/10.1016/j.jfluchem.2017.08.002>.

34. D. Li, M. Liao, Study on the Dehydrofluorination of Vinylidene Fluoride (VDF) and Hexafluoropropylene (HFP) Copolymer. *Polym. Degrad. Stab.* 2018, 152, 116-125. <https://doi.org/10.1016/j.polymdegradstab.2018.04.008>.

35. J.-S. Kim, A. Dutta, V. Vasu, O. I. Adebolu, A. D. Asandei, Universal Group 14 Free Radical Photoinitiators for Vinylidene Fluoride, Styrene, Methyl Methacrylate, Vinyl Acetate, and Butadiene. *Macromolecules* 2019, 52 (22), 8895-8909. <https://doi.org/10.1021/acs.macromol.9b01802>.

36. E. B. Twum, C. Gao, X. Li, E. F. McCord, P. A. Fox, D. F. Lyons, P. L. Rinaldi, Characterization of the Chain-Ends and Branching Structures in Polyvinylidene Fluoride with Multidimensional NMR. *Macromolecules* 2012, 45 (13), 5501-5512. <https://doi.org/10.1021/ma300835s>.

37. B. Ameduri, Copolymers of Vinylidene Fluoride with Functional Comonomers and Applications Therefrom: Recent Developments, Challenges and Future Trends. *Prog. Polym. Sci.* 2022, 133, 101591. <https://doi.org/10.1016/j.progpolymsci.2022.101591>.

38. P. Martins, A. C. Lopes, S. Lanceros-Mendez, Electroactive Phases of Poly(Vinylidene Fluoride): Determination, Processing and Applications. *Prog. Polym. Sci.* 2014, 39 (4), 683-706. <https://doi.org/10.1016/j.progpolymsci.2013.07.006>.

39. L. Ruan, X. Yao, Y. Chang, L. Zhou, G. Qin, X. Zhang, Properties and Applications of the β -Phase Poly (Vinylidene Fluoride). *Polymers* 2018, 10 (3), 228.

40. X. Qian, X. Chen, L. Zhu, Q. M. Zhang, Fluoropolymer Ferroelectrics: Multifunctional Platform for Polar-Structured Energy Conversion. *Science* 2023, 380 (6645), 1-12. <https://doi.org/10.1126/science.adg0902>.

41. P. Qu, X. Liu, S. Wang, C. Xiao, S. Liu, Moderate Dehydrofluorinated PVDF with High Energy Density. *Mater. Lett.* 2018, 221, 275-278. <https://doi.org/10.1016/j.matlet.2018.03.139>.

42. S. Lanceros-Méndez, J. F. Mano, A. M. Costa, V. H. Schmidt, FTIR and DSC Studies of Mechanically Deformed β -PVDF Films. *J. Macromol. Sci.: Part B* 2001, 40 (3-4), 517-527. <https://doi.org/10.1081/MB-100106174>.

- 43.** X. Cai, T. Lei, D. Sun, L. Lin, A Critical Analysis of the α , β and γ Phases in Poly(Vinylidene Fluoride) Using FTIR. *RSC Adv.* 2017, 7 (25), 15382-15389. <https://doi.org/10.1039/C7RA01267E>
- 44.** T. Theophanides, Infrared Spectroscopy-Materials Science, Engineering and Technology Ed. 2012. *IntechOpen*, <https://doi.org/10.5772/2055>.
- 45.** X. Zhang, T. Liu, S. Zhang, X. Huang, B. Xu, Y. Lin, B. Xu, L. Li, C.-W. Nan, Y. Shen, Synergistic Coupling between $\text{Li}_{6.75}\text{La}_3\text{Zr}_{1.75}\text{Ta}_{0.25}\text{O}_{12}$ and Poly(Vinylidene Fluoride) Induces High Ionic Conductivity, Mechanical Strength, and Thermal Stability of Solid Composite Electrolytes. *J. Am. Chem. Soc.* 2017, 139 (39), 13779-13785. <https://doi.org/10.1021/jacs.7b06364>.
- 46.** Y. Bormashenko, R. Pogreb, O. Stanevsky, E. Bormashenko, Vibrational Spectrum of PVDF and Its Interpretation. *Polym. Testing* 2004, 23 (7), 791-796. <https://doi.org/10.1016/j.polymertesting.2004.04.001>
- 47.** H. Dong, K. Xiao, X. Tang, Z. Zhang, J. Dai, R. Long, W. Liao, Preparation and Characterization of Polyurethane (PU)/Polyvinylidene Fluoride (PVDF) Blending Membrane. *Desal. Water Treat.* 2016, 57 (8), 3405-3413. <https://doi.org/10.1080/19443994.2014.988659>.
- 48.** V. E. Zhivulin, R. K. Khairanov, N. A. Zlobina, O. P. Doroshenko, S. E. Evsyukov, I. Y. Doroshenko, L. A. Pesin, Evolution of Molecular Structure of a Dehydrofluorinated Poly(Vinylidene Fluoride) Film During Its Aging. *Results Mater.* 2021, 9, 100163. <https://doi.org/10.1016/j.rinma.2020.100163>.
- 49.** D. Chipara, V. Kuncser, K. Lozano, M. Alcoutlabi, E. Ibrahim, M. Chipara, Spectroscopic Investigations on PVDF- Fe_2O_3 Nanocomposites. *J. Appl. Polym. Sci.* 2020, 137 (30), 48907. <https://doi.org/10.1002/app.48907>
- 50.** V. P. Pavlović, D. Tošić, R. Dojčić, D. Dudić, M. D. Dramićanin, M. Medić, M. M. McPherson, V. B. Pavlović, B. Vlahovic, V. Djoković, PVDF-HFP/NKBT Composite Dielectrics: Perovskite Particles Induce the Appearance of an Additional Dielectric Relaxation Process in Ferroelectric Polymer Matrix. *Polym. Testing* 2021, 96, 107093. <https://doi.org/10.1016/j.polymertesting.2021.107093>
- 51.** D. Chipara, V. Kuncser, K. Lozano, M. Alcoutlabi, E. Ibrahim, M. Chipara, Spectroscopic Investigations on PVDF- Fe_2O_3 Nanocomposites. *J. Appl. Polym. Sci.* 2020, 137 (30), 48907. <https://doi.org/10.1002/app.48907>.
- 52.** L. Muñoz-Fernandez, L. S. Gomez-Villalba, O. Milošević, M. E. Rabanal, Influence of Nanoscale Defects on the Improvement of Photocatalytic Activity of Ag/ZnO. *Mater. Characterization* 2022, 185, 111718. <https://doi.org/10.1016/j.matchar.2021.111718>.

- 53.** M. Pianca, E. Barchiesi, G. Esposito, S. Radice, End Groups in Fluoropolymers. *J. Fluor. Chem.* 1999, 95 (1), 71-84. [https://doi.org/10.1016/S0022-1139\(98\)00304-2](https://doi.org/10.1016/S0022-1139(98)00304-2).
- 54.** S. Tan, X. Hu, S. Ding, Z. Zhang, H. Li, L. Yang, Significantly Improving Dielectric and Energy Storage Properties Via Uniaxially Stretching Crosslinked P(VDF-Co-TrFE) Films. *J. Mater. Chem. A* 2013, 1 (35), 10353-10361. <https://doi.org/10.1039/C3TA11484H>
- 55.** A. Martin, K. Fatyeyeva, L. Truong, A. Daïch, H. Oulyadi, Sulfonation of Polyvinylidene Fluoride: Investigation of the Microstructure by $\{^1\text{H}, ^{13}\text{C}, ^{19}\text{F}\}$ NMR Spectroscopy and Mechanisms. *ACS Appl. Polym. Mater.* 2022, 4 (12), 9463-9471. <https://doi.org/10.1021/acsapm.2c01787>.
- 56.** J. Chen, S. Tan, G. Gao, H. Li, Z. Zhang, Synthesis and Characterization of Thermally Self-Curable Fluoropolymer Triggered by Tempo in One Pot for High Performance Rubber Applications. *Polym. Chem.* 2014, 5 (6), 2130-2141. <https://doi.org/10.1039/C3PY01390A>.
- 57.** Y. Zhang, Y. Zhao, S. Tan, Z. Zhang, Inserting $-\text{CH}=\text{CH}-$ into P(VDF-TrFE) by C-F Activation Mediated with Cu(0) in a Controlled Atom Transfer Radical Elimination Process. *Polym. Chem.* 2017, 8 (11), 1840-1849. <https://doi.org/10.1039/C6PY02119K>.
- 58.** S. Mitra, A. Ghanbari-Siahkali, P. Kingshott, S. Hvilsted, K. Almdal, Chemical Degradation of an Uncrosslinked Pure Fluororubber in an Alkaline Environment. *J. Polym. Sci. Part A: Polym. Chem.* 2004, 42 (24), 6216-6229. <https://doi.org/10.1002/pola.20473>.
- 59.** C. L. Cheng, C. C. Wan, Y. Y. Wang, M. S. Wu, Thermal Shutdown Behavior of PVDF-HFP Based Polymer Electrolytes Comprising Heat Sensitive Cross-Linkable Oligomers. *J. Power Sources* 2005, 144 (1), 238-243. <https://doi.org/10.1016/j.jpowsour.2004.12.043>.
- 60.** C. Van Goethem, M. Mertens, I. F. J. Vankelecom, Crosslinked PVDF Membranes for Aqueous and Extreme pH Nanofiltration. *J. Membr. Sci.* 2019, 572, 489-495. <https://doi.org/10.1016/j.memsci.2018.11.036>.

